

Decreasing magnetization, lithospheric flexure and rejuvenated hydrothermalism off the Japan-Kuril subduction zone

Hanjin Choe, Jerôme Dyment

▶ **To cite this version:**

Hanjin Choe, Jerôme Dyment. Decreasing magnetization, lithospheric flexure and rejuvenated hydrothermalism off the Japan-Kuril subduction zone. Geophysical Research Letters, 2020, 47 (9), pp.e2019GL085975. 10.1029/2019GL085975 . insu-02520688

HAL Id: insu-02520688

https://insu.hal.science/insu-02520688

Submitted on 27 May 2020

HAL is a multi-disciplinary open access archive for the deposit and dissemination of scientific research documents, whether they are published or not. The documents may come from teaching and research institutions in France or abroad, or from public or private research centers.

L'archive ouverte pluridisciplinaire **HAL**, est destinée au dépôt et à la diffusion de documents scientifiques de niveau recherche, publiés ou non, émanant des établissements d'enseignement et de recherche français ou étrangers, des laboratoires publics ou privés.

Geophysical Research Letters

RESEARCH LETTER
10.1029/2019GL085975

Decreasing Magnetization, Lithospheric Flexure, and Rejuvenated Hydrothermalism off the Japan-Kuril Subduction Zone

Hanjin Choe[1] and **Jerome Dyment**[1]

[1]Institut de physique du globe de Paris, Université de Paris, Paris, France

Key Points:
- Decaying seafloor spreading magnetic anomalies are observed before subduction in Japan-Kuril subduction zone
- The damping shape decaying pattern corresponds to increasing heat flow and the hydration of the oceanic crust approaching the trenches
- The extra alteration of magnetic minerals by renewed water circulation from the flexure-related opening of normal faults cause the decay

Correspondence to:
H. Choe,
choe@ipgp.fr

Citation:
Choe, H., & Dyment, J. (2020). Decreasing magnetization, lithospheric flexure, and rejuvenated hydrothermalism off the Japan-Kuril subduction zone. *Geophysical Research Letters*, *45*. https://doi.org/10.1029/2019GL085975

Received 28 OCT 2019
Accepted 16 MAR 2020
Accepted article online 18 MAR 2020

Abstract Seafloor spreading magnetic anomalies formed at mid-ocean ridges initially display strong amplitudes that decay within the first 10 million years as a result of pervasive hydrothermal circulation and alteration. The amplitudes do not vary much for older oceanic crust, suggesting that the thickening sediments hinder heat advection. Here we show, however, that a systematic loss of ~20% in the amplitude of the anomalies arises between the outer rise and the trench on old ocean crust approaching the Japan and Kuril subduction zones. We interpret this decay as reflecting the opening of normal faults and fissures caused by extension on the outer flexural rise and the subsequent renewed circulation of seawater into the oceanic crust, resulting in additional alteration of the magnetic minerals. This interpretation is supported by higher heat flow and seismic velocity changes observed toward the trench.

Plain Language Summary Seafloor spreading magnetic anomalies formed at mid-ocean ridges initially display strong amplitudes that decrease within the first 10 million years as a result of the widespread circulation of hot seawater within the oceanic crust and the resulting alteration of its magnetic minerals. The amplitudes do not vary much for older oceanic crust, suggesting that the thickening sediments hinder the free exchange of seawater between the crustal aquifer and overlying ocean. Here we show, however, that a systematic loss of ~20% in the amplitude of the anomalies appear between the outer rise, an elevation caused by the flexure of the plate entering subduction, and the trench on old ocean crust approaching the Japan and Kuril subduction zones. We interpret this decrease as reflecting the opening of faults and cracks caused by extension at the top of the bent oceanic plate and the subsequent renewed circulation of seawater into the oceanic crust, resulting in additional alteration of the magnetic minerals. This interpretation is supported by higher heat flow and seismic velocity changes observed toward the trench.

1. Introduction

The part of the Pacific plate subducting into the Japan and Kuril subduction zones has been formed at fast spreading rate (70–80 km/My) between Chrons M5 and M17 (e.g., Nakanishi et al., 1989), 124.6–139.7 Ma (Geomagnetic Polarity Time Scale of Malinverno et al., 2012), and is subducting at a rate of 70–90 km/My (Seno, 2017). It is covered with 0.5- to 1.0-km-thick pelagic sediments (Fujie et al., 2016; Tsuru et al., 2002). Satellite-derived free-air gravity anomaly (Sandwell et al., 2014; Figure 1a) clearly shows the Japan and Kuril trenches and two NNW–SSE-trending major fracture zones. A positive, long-wavelength free-air gravity anomaly (~50 mgal) marks the outer rise structure, due to the flexure of the thick oceanic lithosphere approaching subduction zone, ~140-km seaward from the Japan Trench and ~120 km from the Kuril Trench. (Figure 3d). Recent seismic and electromagnetic studies suggest that the normal faults induced by lithospheric flexure at the subduction zone causes increasing hydration of the oceanic lithosphere (Fujie et al., 2018; Key et al., 2012; Ranero et al., 2003).

Magnetic anomalies formed by seafloor spreading initially exhibit strong intensities that decay within the first 10–15 million years as a result of pervasive hydrothermal circulation and alteration (e.g., Dyment et al., 2015). The alteration of the magnetic minerals only takes place where seawater meets the oceanic rocks along cracks and faults (Zhou et al., 2001). After 10–15 Ma, (1) the temperature cools down and the hydrothermal circulation decreases, (2) there is no further generation of cracks and faults, (3) sediments make more difficult the influx of additional seawater, and (4) the existing paths for hydrothermal circulation get gradually clogged (e.g., Hutnak & Fisher, 2007; Lister, 1972). As a result, the magnetic minerals that are

©2020. American Geophysical Union. All Rights Reserved.

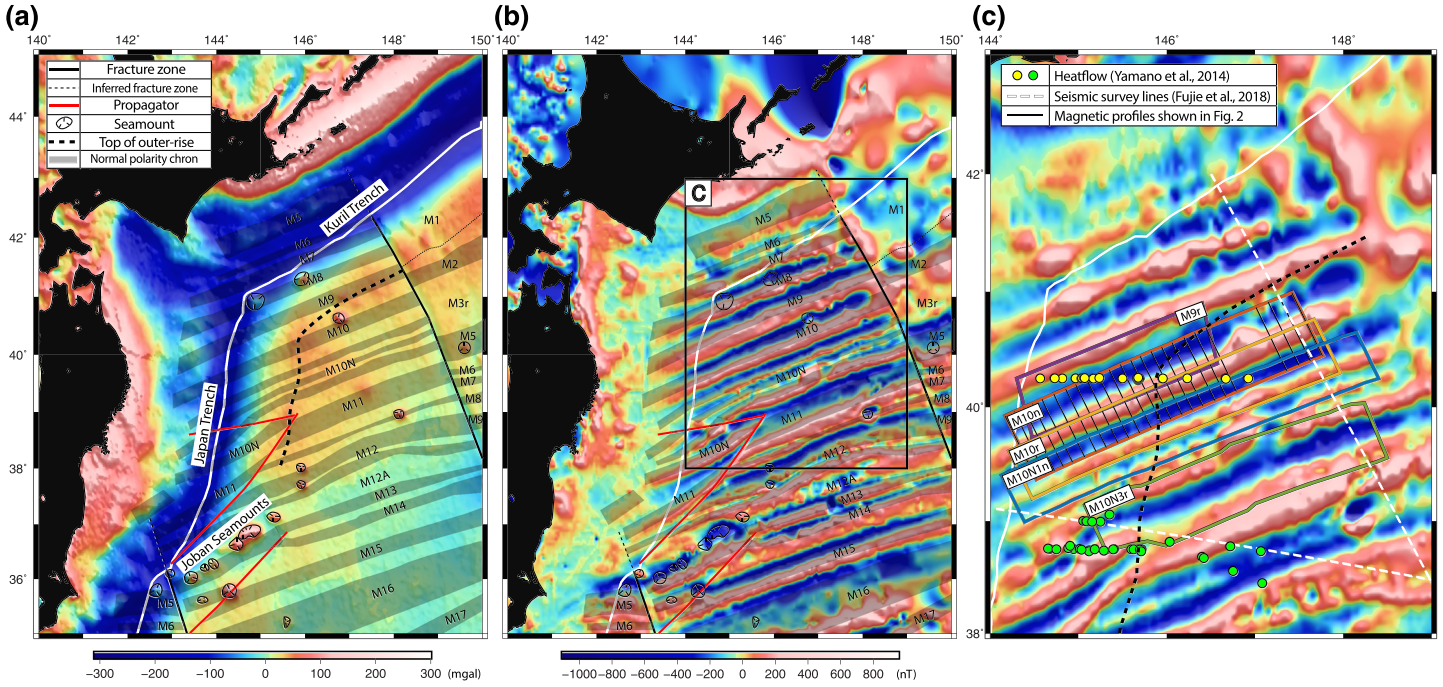


Figure 1. (a) Free-air gravity anomaly map (Sandwell et al., 2014). (b) Magnetic anomaly map in NE Japan. (c) Magnetic anomaly map after reduction to the pole (RTP) in detailed area of investigation. The magnetic anomalies on the oceanic plate trend ENE-WSW, only disrupted by propagators (red lines) and fracture zones (black solid lines). Gray-shaded numbered blocks mark the normal polarity intervals. The Japanese islands are shown in black and the top of outer rise structure by a thick dashed line in (a) and (c). The color boxes in (c) indicate the magnetic anomalies suitable for this study. Yellow and green dots indicate heat flow measurements from two different survey lines from Yamano et al. (2014). White dashed lines indicate seismic profiles from Fujie et al. (2018). The profile across Japan Trench is used in Figure 3c.

accessible to the hydrothermal fluid are fully altered, but those that are out of reach are still bearing a significant magnetization: There is no alteration of additional material and the magnetization of the oceanic crust becomes quite stable, until the magnetic anomaly finally disappear in subduction zones (Okubo et al., 1991).

In a previous work (Choe & Dyment, 2020), we studied the decay of marine magnetic anomalies associated with the subducting slab in the Japan Trench area to evaluate quantitatively the effects of the increasing distance to the magnetic source and thermal demagnetization of the slab (Kido & Fujiwara, 2004; Okubo et al., 1991) using the well-defined slab geometry. While analyzing the same magnetic anomalies prior subduction for reference, we noted that the magnetic anomaly amplitude seems to decrease while approaching the subduction zone. Such a decrease may be due to a deepening basement (i.e., increasing distance to the magnetized source), a geological process, or a combination of both effects.

In this paper, we confirm the systematic decrease of seafloor spreading magnetic anomalies approaching the Japan and Kuril subduction zones by analyzing a high-resolution magnetic anomaly map compiled from the unique scalar and vector marine magnetic anomaly data set available on the area. We ascribe this decrease to rejuvenated hydrothermal circulation and the associated low-temperature alteration induced by flexure-related normal faults and fissures.

2. Data and Methods

In order to make high resolution marine magnetic anomaly map, we collected available magnetic data from the DARWIN database of the Japan Agency for Marine-Earth Science and Technology, the Nautilus database of the Institut Français de Recherche pour l'Exploitation de la MER, and the GEODAS database of the National Center for Environmental Information. The data obtained by proton precession magnetometer were subtracted the International Geomagnetic Reference Field model (Thébault et al., 2015). We applied the method of Isezaki (1986) to correct the data acquired by shipboard three component magnetometer for the ship induced and remanent magnetization and motions. To combine both the proton precession

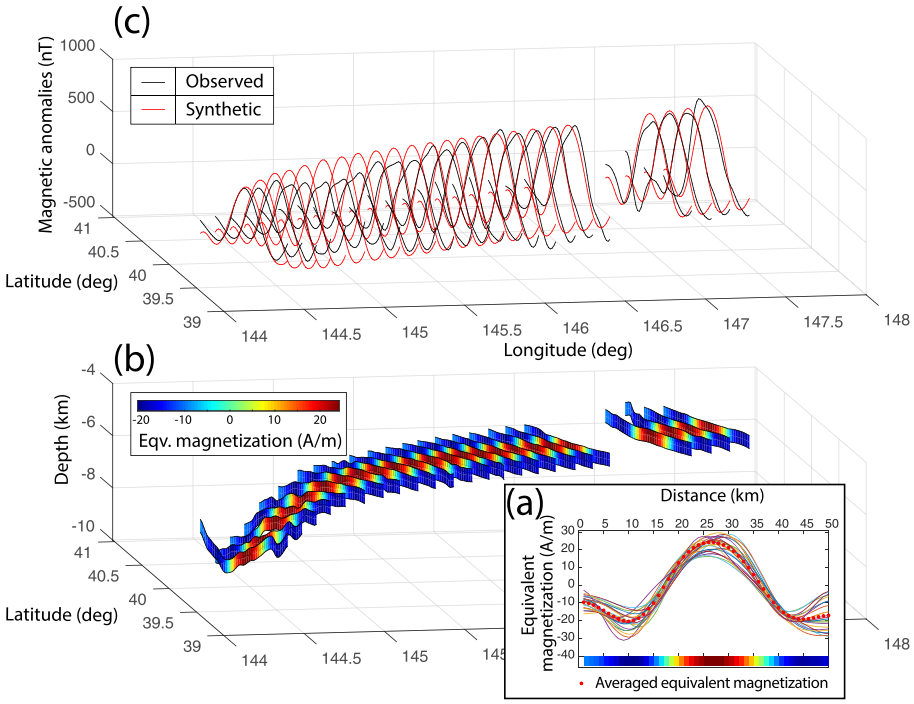


Figure 2. (a) Equivalent magnetization inverted from profiles across magnetic anomaly M10n before subduction (location: see Figure 1c, orange box). Red dotted curve indicates the average equivalent magnetization adopted for further modeling. (b) Three-dimensional view of the source layer and magnetization intensity (color) used to model the synthetic magnetic anomalies. (c) Three-dimensional view of the observed (black) and synthetic (red) magnetic anomalies across magnetic anomaly M10n after subduction (location as above). Comparison of the observed and synthetic anomalies show that the anomaly decreases from 146°E while approaching the trench.

magnetometer and the shipboard three component magnetometer data, the crossover correction algorithm of Choe and Dyment (2020) was applied. We reduced the corrected magnetic anomaly grid to the pole (reduction to the pole) assuming 53.6° inclination and −7.6° declination (International Geomagnetic Reference Field averaged over 20 years), 33° paleoinclination, and 11° paleoazimuth (average value for the study area from the global grids of Dyment & Arkani-Hamed [1998]). Each anomaly profile was inverted to equivalent magnetization assuming a 0.5-km-thick-magnetized source layer with no vertical variation of magnetization (Parker & Huestis, 1974).

We downloaded the bathymetric grid as part of the Global Multiresolution Topography (Ryan et al., 2009) from the Interdisciplinary Earth Data Alliance and the World sediment thickness grid (Divins, 2003) from National Center for Environmental Information. To compute the top of the magnetic source, that is, of the extrusive basalt layer, the sediment thickness grid was subtracted from the bathymetry grid.

To observe a systematic decay of the seafloor spreading magnetic anomalies on oceanic crust approaching the subduction zone, we set the outer flexural rise from the satellite free-air gravity anomaly map (Sandwell et al., 2014) showing a clear flexural rise undisturbed by seamounts or fracture zones (Figure 1c) and computed distances in the WGS84 reference system. We then plotted the ratio of peak to trough anomaly amplitudes of each studied magnetic anomaly versus the distance to the outer flexural rise (Figure 3a).

3. Magnetic Structure of the Subducting Plate Before Entering the Japan-Kuril Trench

The Pacific plate and associated subducting slab display ENE-WSW trending magnetic anomalies of Early Cretaceous age (see above). The southern Kuril Trench is roughly parallel to these anomalies, with anomaly M5 (124.58–126.05 Ma) recognizable although totally subducted whereas anomalies M6 and M7 (127.2–128.54 Ma) are only partially subducted. Conversely, the Japan Trench is oblique to anomalies M8

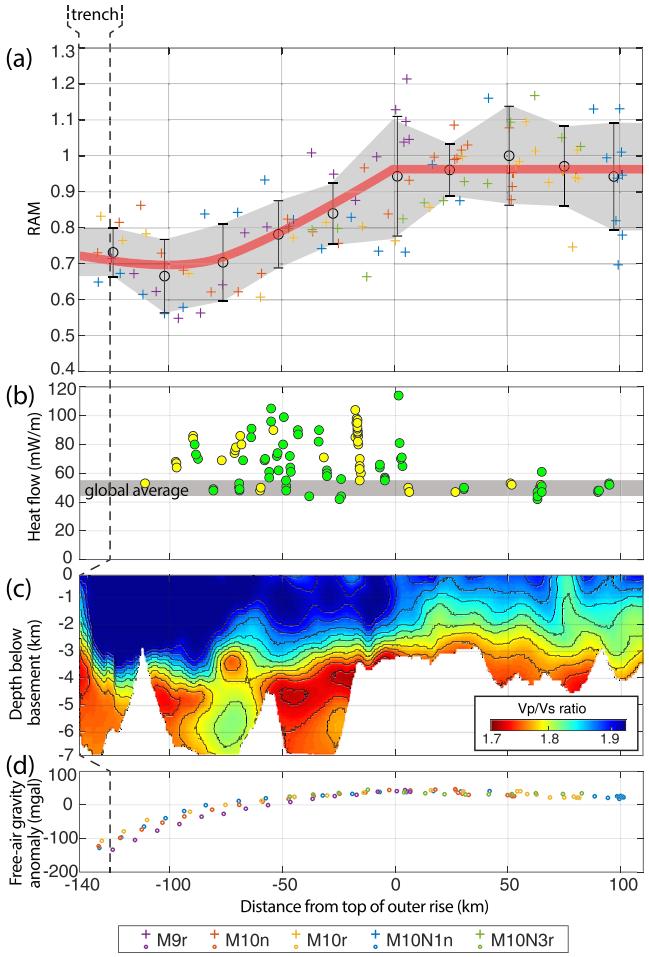


Figure 3. Comparison of the remaining amount of magnetization (RAM) to other geophysical data versus distance to the top of outer rise. (a) RAM. Colored cross signs and dots in a and d correspond to magnetic anomalies shown by boxes of similar color on Figure 1c. Averaged RAM within 25-km distance intervals are shown by circles with error bars, and confidence limits by the shaded area. Thick red line summarized the RAM variation with distance from top of outer rise. (b) Heat flow data (Yamano et al., 2014). Yellow and green dot location is shown in Figure 1c. (c) *Vp*/*Vs* ratio grid from depth below basement (Fujie et al., 2018). Before approaching the top of outer rise, the RAM is close to 0.92, the heat flow converges to global average and *Vp*/*Vs* ratio shows low values. Between the outer rise and the trench, heat flow and *Vp*/*Vs* ratio increase and the RAM decays rapidly as a result of alteration and hydrothermal circulation of magnetic mineral. (d) Free-air gravity anomaly showing the outer rise.

to M11 (128.5–132.67 Ma), which are progressively fading away after passing the Trench to disappear ~100- to 120-km landward (Okubo et al., 1991). These observations result both from the increasing distance to the magnetized source and to thermal demagnetization of the oceanic magnetic layers (Choe & Dyment, 2020). On the plate prior subduction, the magnetic anomalies are slowly fading away while approaching the trench. To evaluate quantitatively the amplitude variation of these anomalies, we selected data showing clear seafloor spreading magnetic anomalies both in amplitude and wavelength (i.e., 20–40 km), in areas of dense data coverage and spanning from outer rise to trench. Profiles perturbed by local complexities such as seamounts, propagators, and fracture zones are discarded.

Investigating the same anomaly reduces possible biases related to paleomagnetic field intensity variation with time. We limited our study to magnetic anomalies M9r to M10Nr (129.7–132.0 Ma) off the Japan Trench. We compared the observed magnetic anomaly profiles to synthetic ones computed by assuming that (1) the basement is the top of a 0.5-km-thick--magnetized extrusive basalt layer and (2) the magnetization is the average of all equivalent magnetization profiles inverted from the observed anomaly profiles with the same local geometry. Figure 2 presents the example of magnetic anomaly M10n (133.45–133.49 Ma), which shows a good fit between the observed and synthetic anomalies East of the outer rise and an increasing misfit between the outer rise and the trench (Figure 2c). We computed the ratio of peak to trough anomaly amplitudes of the observed and synthetic anomalies, hereafter named RAM (remaining amount of magnetization). Figure 3a represents the RAM versus the distance to the closest outer rise for all anomalies and, despite some scatter, shows a significant decrease of the RAM toward the trench. We averaged the RAM at 25-km intervals and adopted the corresponding standard deviation as the uncertainty (Figure 3a). The average RAM is constant at 0.95 east of the outer rise and decreases exponentially to 0.72 from the outer rise to the trench (Figure 3a).

The decreasing RAM reflects a loss of magnetization occurring between the outer rise and the trench and can be attributed to two main processes, the alteration and thermal demagnetization of magnetic minerals.

4. Decay of Magnetization Before Subduction: Alteration as the Main Process

Two major processes can be inferred to explain the decay of marine magnetic anomalies between the outer rise and the trench. The first one, thermal demagnetization, relates the loss of magnetization to an increase of temperature: The magnetic minerals are heated beyond their Curie temperature and loose their magnetization (Okubo et al., 1991). The second process, alteration, considers that hydrothermal circulation oxidizes the magnetic minerals which transform to less or nonmagnetic minerals (Dyment et al., 2015; Tivey et al., 1993).

Moreover, recent heat flow data show values close to the global average (~50 mW/m^2) east of the outer rise and scattered, in average higher values between the outer rise and the trench (Yamano et al., 2014; Figure 3 b). The higher heat flow observed over the oceanic crust approaching the trench suggests high temperatures that may support thermal demagnetization of titanomagnetite, the magnetic bearer of extrusive basalt that exhibits a strong magnetic intensity but a low Curie temperature (150–350 °C; Zhou et al., 2001; Gee & Kent, 2007). However, a recently published thermal structure model (Kawada et al., 2014) concluded that the additional hydrothermal circulation which causes the higher and more scattered heat flow measurements of

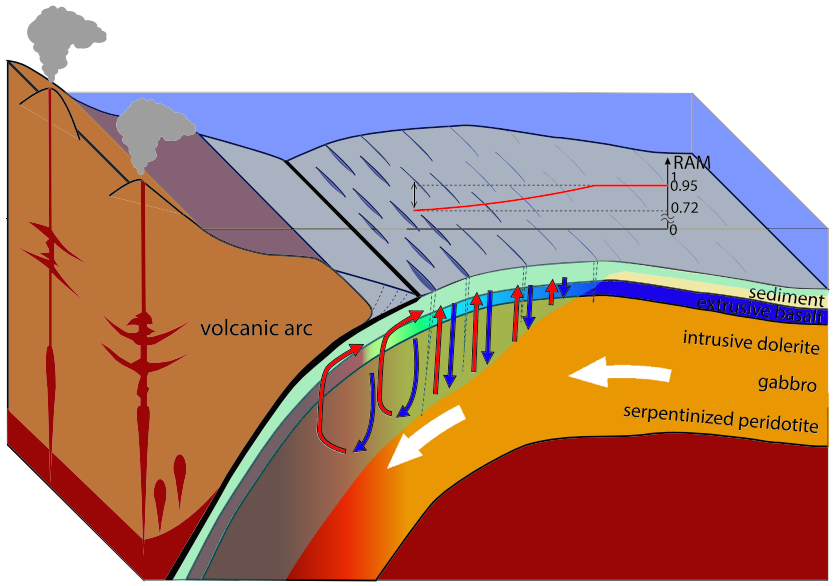


Figure 4. Schematic illustration of the processes shaping the magnetic structure of the subducting plate. Red solid line describes the RAM decrease shown in Figure 3a. Blue and red arrows describe hydrothermal activity in the oceanic crust. Before subduction, normal faults induced by the bending of old oceanic lithosphere causes seawater penetration and active hydrothermal activity and in turn oxidation of the magnetic minerals and crustal magnetization reduction. Once entered in subduction, the heat mined by hydrothermal circulation does not escape to the ocean as a result of thermal blanketing by the accretionary prism, the pelagic sediments and the possibly impermeable decollement surface, making the temperature increase and the magnetization of the extrusive layer then the deeper crust fade away as their magnetic minerals pass their Curie temperature.

Yamano et al. (2014) only heats up the oceanic crust at 1.5-km depth by 40 °C, insufficient to reach the Curie temperature and significantly demagnetize the plate. We therefore consider that thermal demagnetization only plays a minor role in the observed decay of the marine magnetic anomalies before entering subduction.

Recent active seismic reflection profiles show that the *Vp*/*Vs* ratio strongly increases and the high *Vp*/*Vs* layer thickens up to 3.5-km-deep below seafloor from the outer rise to the trench (Fujie et al., 2018; Figure 3c). These results and the heat flow measurements (Yamano et al., 2014) support rejuvenation of the hydrothermal circulation within the old oceanic crust. Both vertical and lateral circulations may participate to the alteration of magnetic minerals resulting in the observed decrease of magnetization. Even though alteration bands have not been observed by seismics in the area, the earthquakes distribution in the outer trench wall (e.g., Obana et al., 2012) and increasing bathymetric roughness toward the trench (e.g., Nakanishi, 2011) show that the bending faults develop as they approach the trench, as observed by active seismics in most subduction zones (Contreras-Reyes et al., 2008; Fujie et al., 2018; Shillington et al., 2015). Conversely, flexure also results in increasing the bulk permeability of the oceanic crust, allowing lateral flow driven by the buoyancy of warming fluids (Harris et al., 2017; Spinelli & Wang, 2008; Yamano et al., 2014) as the aquifer enters subduction and deepens (Kawada et al., 2014). Clearly magnetic anomalies are of limited help to discriminate between the two styles of fluid flow.

The decay of RAM is therefore most likely caused by alteration of magnetic minerals due to rejuvenated hydrothermal circulation as the lithosphere flexes in response to subduction (Figure 4). It is interesting to note that the decay seems to attenuate from the outer rise to the trench, as does the increasing crustal hydration estimated from *Vp*/*Vs* values (Figure 3c): From the outer rise (km 0) to about km 80, the RAM decreases rapidly from 0.95 to 0.7 and the limit between low and high *Vp*/*Vs* ratio rapidly deepens from ~1 to 3 km, whereas between km 80 and the trench, the RAM is almost constant at 0.7 and the limit between low and high *Vp*/*Vs* ratio is about 4 km. Both the crustal hydration and the magnetic mineral alteration are fast when the faults and fissure open and the porosity increases and tend to saturate with time, when hydrated and altered minerals cover the cracks and their vicinity. For this reason, the RAM decay is much more subdued near the trench (Figure 3a).

5. An Integrated Magnetization Model of the Subducting Plate

This study and our previous work (Choe & Dyment, 2020) offer an integrated view on the magnetic structure of the Pacific Plate before and after entering subduction in the Japan-Kuril Trench. Here we show that after passing the outer rise, the magnetic anomaly amplitude decreases by roughly 20% due to the alteration of magnetic minerals induced by rejuvenated hydrothermal circulation. From our previous study, half of the remaining 80% is further erased between 9 and 12 km depth of the slab surface below sea level due to the thermal demagnetization of the extrusive basalt layer above the Curie temperature of titanomagnetites (150–350 °C). The last 40% are finally removed between 12 and 20 km depth of the slab surface below sea level by thermal demagnetization of the deeper crust above the Curie temperature of magnetite (580 °C; Gee & Kent, 2007).

Heat flow, *Vp*/*Vs* structure, and magnetization decay concur in supporting rejuvenated hydrothermal circulation and the subsequent alteration as an important process on the plate before subduction. As a consequence, the crust entering subduction is already very altered, and it is therefore unlikely that the drop of magnetization observed between 9 and 12 km may be due to any vigorous hydrothermalism and alteration. Thermal demagnetization appears as the only process able to generate such a magnetization drop. A major difference between the oceanic crust before and after subduction is that the heat mined by hydrothermal circulation before subduction is partly released to the ocean by conduction and seawater infiltrates into the basement along the bending faults as they develop toward the trench (Boston et al., 2014; Nakanishi, 2011; Obana et al., 2012). The thermal structure is only marginally affected, as noted by Kawada et al. (2014). Conversely, after subduction, no new seawater infiltrates the system. The seawater trapped in the thick aquifer of Kawada et al. (2014) continues to mine the heat from depth but can only escape laterally due to the overlying accretionary prism, pelagic sediments and the possibly impermeable decollement surface, resulting in the same fluid convecting and heating the oceanic crust by thermal blanketing (Granot & Dyment, 2019). As a result, the heat flow measured on the overriding plate is low (Kawada et al., 2014; Yamano et al., 2014).

Our study underlines the major role of fluid circulation, alteration, and more generally of thermodynamics in shaping the Japan-Kuril Trench before and after subduction. In predicting a warmer subduction zone, these results have consequences on the depth and location of the seismogenic zone, which knowledge is important to assess the seismic risk in the area (Choe & Dyment, 2020). Magnetic anomalies reflect thermal processes and can be used as a tool to address these processes. Our inferences on the thermodynamics of subduction zones should be confirmed by a rigorous thermal model that is beyond the scope of this paper.

Acknowledgments
We thank Nobukazu Seama and an anonymous reviewer for their helpful comments, as well as Editor Monika Korte for her efficient handling of this paper. H. C. has been supported by a fellowship of Ecole Doctorale STEP'UP. We thank all scientists and crews who collected the marine geophysical data used in this study. This is IPGP contribution 4126. The marine magnetic data used in this study are available at the National Center for Environmental Information (GEODAS database, https://www.ngdc.noaa.gov/mgg/geodas/trackline.html), Japan Agency for Marine-Earth Science and Technology (DARWIN database, http://www.godac.jamstec.go.jp/darwin/e), and Institut Français de Recherche pour l'Exploitation de la MER (Nautilus, https://www.flotteoceanographique.fr/en/Cruises/Research/Oceanographic-campaigns-data).

References

Boston, B., Moore, G. F., Nakamura, Y., & Kodaira, S. (2014). Outer-rise normal fault development and influence on near-trench décollement propagation along the Japan trench, off Tohoku. *Earth, Planets and Space*, *66*(1), 1–17. https://doi.org/10.1186/1880-5981-66-135

Choe, H., & Dyment, J. (2020). Fading magnetic anomalies, thermal structure and earthquakes in the Japan Trench. *Geology*, *48*(3), 278–282. https://doi.org/10.1130/G46842.1

Contreras-Reyes, E., Grevemeyer, I., Flueh, E. R., & Reichert, C. (2008). Upper lithospheric structure of the subduction zone offshore of southern Arauco peninsula, Chile, at ∼38°S. *Journal of Geophysical Research*, *113*, B07303. https://doi.org/10.1029/2007JB005569

Divins, D.L. (2003). Total sediment thickness of the world's oceans and marginal seas, NOAA National Geophysical Data Center, Boulder (available at https://www.ngdc.noaa.gov/mgg/sedthick/sedthick.html).

Dyment, J., & Arkani-Hamed, J. (1998). Contribution of lithospheric remanent magnetization to satellite magnetic anomalies over the World's oceans. *Journal of Geophysical Research*, *103*(B7), 15,423–15,441. https://doi.org/10.1029/97JB03574

Dyment, J., Choi, Y., Hamoudi, M., Lesur, V., & Thebault, E. (2015). Global equivalent magnetization of the oceanic lithosphere. *Earth and Planetary Science Letters*, *430*, 54–65. https://doi.org/10.1016/j.epsl.2015.08.002

Fujie, G., Kodaira, S., Kaiho, Y., Yamamoto, Y., Takahashi, T., Miura, S., & Yamada, T. (2018). Controlling factor of incoming plate hydration at the north-western Pacific margin. *Nature Communications*, *9*(1), 3844. https://doi.org/10.1038/s41467-018-06320-z

Fujie, G., Kodaira, S., Sato, T., & Takahashi, T. (2016). Along-trench variations in the seismic structure of the incoming Pacific plate at the outer rise of the northern Japan trench. *Geophysical Research Letters*, *43*, 666–673. https://doi.org/10.1002/2015GL067363

Gee, J. S., & Kent, D. V. (2007). Source of oceanic magnetic anomalies and the geomagnetic polarity timescale. In *Treatise on Geophysics*, (Vol. 5, pp. 455–507). Elsevier. https://doi.org/10.1016/B978-044452748-6.00097-3

Granot, R., & Dyment, J. (2019). The influence of post-accretion sedimentation on marine magnetic anomalies. *Geophysical Research Letters*, *46*, 4645–4652. https://doi.org/10.1029/2019GL082265

Harris, R. N., Spinelli, G. A., & Fisher, A. T. (2017). Hydrothermal circulation and the thermal structure of shallow subduction zones. *Geosphere*, *13*(5), 1425–1444. https://doi.org/10.1130/GES01498.1

Hutnak, M., & Fisher, A. T. (2007). Influence of sedimentation, local and regional hydrothermal circulation, and thermal rebound on measurements of seafloor heat flux. *Journal of Geophysical Research*, *112*, B12101. https://doi.org/10.1029/2007JB005022

Isezaki, N. (1986). A new shipboard three-component magnetometer. *Geophysics*, *51*(10), 1992–1998. https://doi.org/10.1190/1.1442054

Kawada, Y., Yamano, M., & Seama, N. (2014). Hydrothermal heat mining in an incoming oceanic plate due to aquifer thickening: Explaining the high heat flow anomaly observed around the Japan Trench. *Geochemistry, Geophysics, Geosystems*, *15*, 1580–1599. https://doi.org/10.1002/2014GC005285

Key, K., Constable, S., Matsuno, T., Evans, R. L., & Myer, D. (2012). Electromagnetic detection of plate hydration due to bending faults at the Middle America Trench. *Earth and Planetary Science Letters*, *351–352*(May 2019), 45–53. https://doi.org/10.1016/j.epsl.2012.07.020

Kido, Y., & Fujiwara, T. (2004). Regional variation of magnetization of oceanic crust subducting beneath the Nankai Trough. *Geochemistry, Geophysics, Geosystems*, *5*, Q03002. https://doi.org/10.1029/2003GC000649

Lister, C. R. B. (1972). On the thermal balance of a mid-ocean ridge. *Geophysical Journal International*, *26*(5), 515–535. https://doi.org/10.1111/j.1365-246X.1972.tb05766.x

Malinverno, A., Hildebrandt, J., Tominaga, M., & Channell, J. E. T. (2012). M-sequence geomagnetic polarity time scale (MHTC12) that steadies global spreading rates and incorporates astrochronology constraints. *Journal of Geophysical Research*, *117*, B06104. https://doi.org/10.1029/2012JB009260

Nakanishi, M. (2011). Bending-related topographic structures of the subducting plate in the Northwestern Pacific Ocean. In Y. Ogawa, R. Anma, & Y. Dilek (Eds.), *Accretionary Prisms and Convergent Margin Tectonics in the Northwest Pacific Basin*, (Vol. 8, pp. 1–38). Springer. https://doi.org/10.1007/978-90-481-8885-7

Nakanishi, M., Tamaki, K., & Kobayashi, K. (1989). Mesozoic magnetic anomaly lineations and seafloor spreading history of the northwestern Pacific. *Journal of Geophysical Research*, *94*(B11), 15,437–15,462. https://doi.org/10.1029/JB094iB11p15437

Obana, K., Fujie, G., Takahashi, T., Yamamoto, Y., Nakamura, Y., Kodaira, S., et al. (2012). Normal-faulting earthquakes beneath the outer slope of the Japan Trench after the 2011 Tohoku earthquake: Implications for the stress regime in the incoming Pacific plate. *Geophysical Research Letters*, *39*, L00G24. https://doi.org/10.1029/2011GL050399

Okubo, Y., Makino, M., & Kasuga, S. (1991). Magnetic model of the subduction zone in the northeast Japan Arc. *Tectonophysics*, *192*(1–2), 103–115. https://doi.org/10.1016/0040-1951(91)90249-R

Parker, R. L., & Huestis, S. P. (1974). The inversion of magnetic anomalies in the presence of topography. *Journal of Geophysical Research*, *79*(11), 1587–1593. https://doi.org/10.1029/JB079i011p01587

Ranero, C. R., Morgan, J. P., McIntosh, K., & Reichert, C. (2003). Bending-related faulting and mantle serpentinization at the Middle America trench. *Nature*, *425*(6956), 367–373. https://doi.org/10.1038/nature01961

Ryan, W. B. F., Carbotte, S. M., Coplan, J. O., O'Hara, S., Melkonian, A., Arko, R., et al. (2009). Global multi-resolution topography synthesis. *Geochemistry, Geophysics, Geosystems*, *10*, Q03014. https://doi.org/10.1029/2008GC002332

Sandwell, D. T., Müller, R. D., Smith, W. H. F., Garcia, E., & Francis, R. (2014). New global marine gravity model from CryoSat-2 and Jason-1 reveals buried tectonic structure. *Science*, *346*(6205), 65–67. https://doi.org/10.1126/science.1258213

Seno, T. (2017). Subducted sediment thickness and *Mw* 9 earthquakes. *Journal of Geophysical Research: Solid Earth*, *122*, 470–491. https://doi.org/10.1002/2016JB013048

Shillington, D. J., Bécel, A., Nedimović, M. R., Kuehn, H., Webb, S. C., Abers, G. A., et al. (2015). Link between plate fabric, hydration and subduction zone seismicity in Alaska. *Nature Geoscience*, *8*(12), 961–964. https://doi.org/10.1038/ngeo2586

Spinelli, G. A., & Wang, K. (2008). Effects of fluid circulation in subducting crust on Nankai margin seismogenic zone temperatures. *Geology*, *36*(11), 887–890. https://doi.org/10.1130/G25145A.1

Thébault, E., Finlay, C. C., Beggan, C. D., Alken, P., Aubert, J., Barrois, O., et al. (2015). International geomagnetic reference field: The 12th generation. *Earth, Planets and Space*, *67*(1), 79. https://doi.org/10.1186/s40623-015-0228-9

Tivey, M. A., Rona, P. A., & Schouten, H. (1993). Reduced crustal magnetization beneath the active sulfide mound, TAG hydrothermal field, Mid-Atlantic Ridge at 26°N. *Earth and Planetary Science Letters*, *115*(1–4), 101–115. https://doi.org/10.1016/0012-821X(93)90216-V

Tsuru, T., Park, J.-O., Miura, S., Kodaira, S., Kido, Y., & Hayashi, T. (2002). Along-arc structural variation of the plate boundary at the Japan Trench margin: Implication of interplate coupling. *Journal of Geophysical Research*, *107*(B12), 2357. https://doi.org/10.1029/2001JB001664

Yamano, M., Hamamoto, H., Kawada, Y., & Goto, S. (2014). Heat flow anomaly on the seaward side of the Japan Trench associated with deformation of the incoming Pacific plate. *Earth and Planetary Science Letters*, *407*, 196–204. https://doi.org/10.1016/j.epsl.2014.09.039

Zhou, W., Van der Voo, R., Peacor, D. R., Wang, D., & Zhang, Y. (2001). Low-temperature oxidation in MORB of titanomagnetite to titanomaghemite: A gradual process with implications for marine magnetic anomaly amplitudes. *Journal of Geophysical Research*, *106*(B4), 6409–6421. https://doi.org/10.1029/2000JB900447